# Critical line of $2 + 1$ flavor QCD

Paolo Cea[*]

*Dipartimento di Fisica dell'Università di Bari and INFN - Sezione di Bari, I-70126 Bari, Italy*

Leonardo Cosmai[†]

*INFN - Sezione di Bari, I-70126 Bari, Italy*

Alessandro Papa[‡]

*Dipartimento di Fisica dell'Università della Calabria and INFN - Gruppo collegato di Cosenza,
I-87036 Arcavacata di Rende, Cosenza, Italy*

We determine the curvature of the (pseudo)critical line of QCD with $n_f = 2 + 1$ staggered fermions at nonzero temperature and quark density by analytic continuation from imaginary chemical potentials. Monte Carlo simulations are performed by adopting the highly improved staggered quarks /tree action discretization, as implemented in the code by the MILC Collaboration, suitably modified to include a nonzero imaginary baryon chemical potential. We work on a line of constant physics, as determined in Ref. [1], adjusting the couplings so as to keep the strange quark mass $m_s$ fixed at its physical value, with a light to strange mass ratio of $m_l/m_s = 1/20$. In the present investigation, we set the chemical potential at the same value for the three quark species, $\mu_l = \mu_s \equiv \mu$. We explore lattices of different spatial extensions, $16^3 \times 6$ and $24^3 \times 6$, to check for finite size effects, and present results on a $32^3 \times 8$ lattice, to check for finite cutoff effects. We discuss our results for the curvature $\kappa$ of the (pseudo)critical line at $\mu = 0$, which indicate $\kappa = 0.018(4)$, and compare them with previous lattice determinations by alternative methods and with experimental determinations of the freeze-out curve.

## I. INTRODUCTION

It is now well established that quantum chromodynamics (QCD) is the theory underlying strong interactions. As such, it must be able to account for the different phases of strongly interacting matter under usual or unusual (extreme) conditions. In particular, a transition or rapid crossover is thought to exist from a low-temperature hadronic phase to a high-temperature quark-gluon plasma (QGP) phase; the line separating these two phases in the temperature-baryon density plane is called the QCD (pseudo)critical line and has been the subject of many theoretical investigations.

Determining the exact location of this line and the nature of the transition across it has many important theoretical and phenomenological implications, which go from the physics of the early Universe, corresponding to the high $T$ and low baryon density region of the phase diagram, to the physics of the interior of some compact astrophysical objects, corresponding to the low $T$ and high baryon density region. Moreover, various experiments have been devised or have been planned in order to study this transition under controlled conditions in a laboratory, via heavy-ion collisions at ultrarelativistic energies.

Depending on the beam energy, different conditions of temperature and baryon density can be realized in the fireball produced after the collision, such that the QGP phase appears as a transient state, before the system freezes out and partons recombine into hadrons. For a given collision energy, the particle yields are found to be well described by a thermal-statistical model assuming approximate chemical equilibrium, as realized at the chemical freeze-out point, in terms of only two parameters: the freeze-out temperature $T$ and the baryon chemical potential $\mu_B$. The set of freeze-out parameters determined in experiments with different collision energies lies on a curve in the $(T, \mu_B)$ plane, extending up to $\mu_B \lesssim 800$ MeV (see Fig. 1 of Ref. [2], or Ref. [3] for a recent reanalysis of experimental data).

There is no compelling reason for the chemical freeze-out curve and the QCD (pseudo)critical line to coincide. Chemical freeze-out is reached as the fireball cools down, subsequently to rehadronization. Hence, the only assumption that can be made *a priori* is that the freeze-out curve lies below the (pseudo)critical line in the $\mu_B$-$T$ plane. However, a reasonable guess is that chemical freeze-out is reached shortly after hadronization, so that the two curves lie close to each other. In general, the QCD (pseudo)critical line, as well as the freeze-out curve, can be parametrized, at low baryon densities, by a lowest order Taylor expansion in the baryon chemical potential, as follows:

---
[*]paolo.cea@ba.infn.it
[†]leonardo.cosmai@ba.infn.it
[‡]papa@cs.infn.it

$$\frac{T(\mu_B)}{T_c(0)} = 1 - \kappa \left( \frac{\mu_B}{T(\mu_B)} \right)^2, \qquad (1)$$

where $T_c(0)$ is the (pseudo)critical temperature at vanishing baryon density.

Within QCD, a first-principle approach aimed at locating the (pseudo)critical line by means of numerical simulations on a space-time lattice is unfeasible at nonzero baryon density, due to the well-known "sign problem": the QCD fermion determinant becomes complex and the probability interpretation of the measure of the Euclidean path integral, which is necessary for the application of standard Monte Carlo importance sampling, is lost.

Several methods have been invented to attack this problem at an algorithmic level or to circumvent it (for a review, see Ref. [4]): reweighting from the ensemble at $\mu_B = 0$ [5], the Taylor expansion method [6], the canonical approach [7–9], the density of states method [10] and the method of analytic continuation from an imaginary chemical potential [11–22].

A comparison among different approaches has been possible only in a few cases. QCD with $n_f = 4$ in the standard staggered formulation, discretized on $N_t = 4$ lattices with a bare quark mass $am = 0.05$, has been the laboratory for many investigations: in that case, the transition is first order all the way along the critical line, and all methods agree in the range $\mu_B/(3T) \lesssim 1$ (see Refs. [9,23] and Fig. 8 of Ref. [15]). No such direct comparisons exist for $n_f = 2$ QCD; however, different discretizations with unphysical quark masses lead to compatible results (see, e.g., the discussion in Sec. 3 of Ref. [17]).

The situation in QCD with $n_f = 2 + 1$ and physical or almost-physical quark masses deserves a more detailed discussion. It is now widely accepted that the transition at $\mu_B = 0$ is a smooth crossover [24], thus implying that the determination of the transition temperature $T_c$ and the curvature of the (pseudo)critical line depend on the observable adopted to probe the transition. Indeed, with particular reference to the curvature $\kappa$ defined in Eq. (1), the Budapest-Wuppertal Collaboration [25], using a Symanzik improved gauge action and stout-link improved staggered fermions on lattices with temporal size $N_t = 6, 8, 10$ and aspect ratios equal to three and four, finds, after continuum extrapolation, $\kappa = 0.0089(14)$ by the Taylor expansion method with the strange quark number susceptibility as probe observable and $\kappa = 0.0066(20)$ when, instead, the renormalized chiral condensate is used. The Bielefeld-BNL Collaboration [26], using the p4 action on lattices with $N_t = 4$ and 8, and aspect ratios up to four, finds $\kappa = 0.0066(7)$ again with the Taylor expansion method and the light-quark susceptibility as a probe observable. Another collaboration [27] adopted improved staggered fermions in the p4fat3 version, on lattices with $N_t = 4$ and aspect ratio four with physical strange quark mass and pion mass at 220 MeV, getting $\kappa = 0.0100(2)$ by the method of analytic continuation, with the Polyakov loop phase as a probe.

The comparison of these results for the curvature $\kappa$ with those obtained for the freeze-out curve and coming from the experiments with heavy-ion collisions is far from satisfactory. According to the analysis of Ref. [2], the curvature $\kappa$ of the freeze-out curve is a factor 2 to 3 higher than the above lattice determinations, even if a recent reanalysis [3], which includes the effects of inelastic collisions taking place after freeze-out, seems to reduce the value of $\kappa$, bringing it into better agreement with existing lattice results.

In such a situation, a new, independent lattice determination of the QCD (pseudo)critical line at small baryon densities could provide us with useful additional information and help us identify possible sources of systematic uncertainties in the theoretical determination of the (pseudo)critical line. Indeed, while systematic effects within each single method trying to circumvent the sign problem may seem to be well under control, it is only the comparison between different independent methods which could provide a clear final picture.

The aim of this work is to have a first estimate of the QCD (pseudo)critical line by the method of analytic continuation, using the HISQ/tree action of the MILC Collaboration with $2 + 1$ staggered fermions, properly modified to be endowed with an imaginary chemical potential that is common to each fermion. The strange mass is set at the physical value, and simulations are performed on the line of constant physics (LCP) with the light-quark mass fixed at $m_l = m_s/20$, as determined in Ref. [1]. As for quark chemical potentials, in the present study we assign the same value to the three quark species, $\mu_l = \mu_s \equiv \mu$. This choice is certainly the most convenient for studying the theory at imaginary chemical potentials, since it leads to a simpler structure of the phase diagram for negative values of $\mu^2$. For the comparison with the freeze-out curve, settings with $\mu_s \neq \mu_l$ should also be taken into account. We plan to consider this issue in forthcoming studies. We explore lattices of different spatial extensions, $16^3 \times 6$ and $24^3 \times 6$, to check for finite size effects, and present results on a $32^3 \times 8$ lattice, to check for finite cutoff effects.

## II. SIMULATION DETAILS AND NUMERICAL RESULTS

We perform simulations of lattice QCD with $2 + 1$ flavors of rooted staggered quarks at imaginary quark chemical potential. We have made use of the HISQ/tree action [28,29] as implemented in the publicly available MILC code [30], which has been suitably modified by us in order to introduce an imaginary quark chemical potential, $\mu = \mu_B/3$. That has been done by multiplying all forward and backward temporal links entering the discretized Dirac operator by $\exp(ia\mu)$ and $\exp(-ia\mu)$, respectively: in this way, the fermion determinant is still real and positive, so that standard Monte Carlo methods can be applied. As mentioned above, in the present study we have

$\mu = \mu_l = \mu_s$. All simulations make use of the rational hybrid Monte Carlo (RHMC) algorithm. The length of each RHMC trajectory has been set to 1.0 in molecular dynamics time units.

We have simulated QCD at finite temperature and imaginary quark chemical potential on lattices of size $16^3 \times 6$, $24^3 \times 6$, and $32^3 \times 8$. In particular, most simulations have been performed on the smallest lattice, while for $\mu/(\pi T) = 0.2i$ we have also considered a $24^3 \times 6$ lattice and a $32^3 \times 8$ lattice, in order to check for finite size and for finite cutoff effects. We have typically discarded not less than 1000 trajectories for each run and have collected from 4000 to 8000 trajectories for measurements.

The (pseudo)critical line $\beta_c(\mu^2)$ has been determined as the value for which the disconnected susceptibility of the light-quark chiral condensate exhibits a peak. To precisely localize the peak, a Lorentzian fit has been used. For the $24^3 \times 6$ and $32^3 \times 8$ lattices, the values of the susceptibility at $\mu/(\pi T) = 0$ have been taken from Table X and Table XI of Ref. [1], respectively. For the reader's convenience, we summarize in Table I the (pseudo)critical couplings obtained by the Lorentzian fit for the different values of the chemical potential and lattice size used in this work. For illustrative purposes, in Fig. 1 we display our determination of the (pseudo)critical couplings at $\mu/(\pi T) = 0.2i$ for $16^3 \times 6$, $24^3 \times 6$, and $32^3 \times 8$ lattices. We notice that the discrepancy in the determination of $\beta_c$ on the $16^3 \times 6$ and the $24^3 \times 6$ lattices, which may indicate the presence of finite size effects, will be strongly suppressed when considering the ratio of temperatures, $T_c(\mu)/T_c(0)$.

To determine the ratio $T_c(\mu)/T_c(0)$, we need to set the lattice spacing. This is done following the discussion in Appendix B of Ref. [1], where, for this particular value of $m_l/m_s$, the spacing is given in terms of the $r_1$ parameter:

$$\frac{a}{r_1}(\beta)_{m_l=0.05m_s} = \frac{c_0 f(\beta) + c_2 (10/\beta) f^3(\beta)}{1 + d_2 (10/\beta) f^2(\beta)}, \qquad (2)$$

TABLE I. Summary of the values of the (pseudo)critical couplings $\beta_c$ for the imaginary quark chemical potentials $\mu$ considered in this work. The data for $\mu = 0$ on the $24^3 \times 6$ lattice and on the $32^3 \times 6$ lattice have been estimated from the disconnected chiral susceptibilities reported, respectively, on Table X and Table XI of Ref. [1].

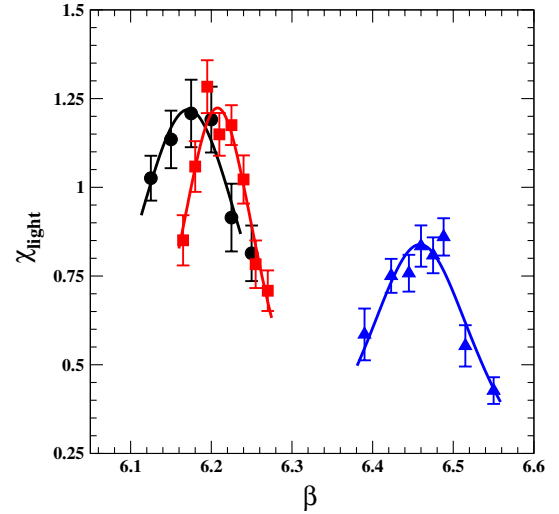| Lattice | $\mu/(\pi T)$ | $\beta_c$ | $T_c(\mu)/T_c(0)$ |
|---|---|---|---|
| $16^3 \times 6$ | 0. | 6.102(8) | 1.000 |
| | 0.15i | 6.147(10) | 1.045(13) |
| | 0.2i | 6.171(12) | 1.070(15) |
| | 0.25i | 6.193(14) | 1.093(17) |
| $24^3 \times 6$ | 0. | 6.148(8) | 1.000 |
| | 0.2i | 6.208(5) | 1.060(10) |
| $32^3 \times 8$ | 0. | 6.392(5) | 1.000 |
| | 0.2i | 6.459(9) | 1.068(11) |



FIG. 1 (color online). The real part of the disconnected susceptibility of the light-quark chiral condensate for $16^3 \times 6$ and $24^3 \times 6$ (full circles and full squares, respectively) and for $32^3 \times 8$ (full triangles) at $\mu/(\pi T) = 0.2i$. Full lines are the fits to the peaks using a Lorentzian.

with $c_0 = 44.06$, $c_2 = 272102$, $d_2 = 4281$, $r_1 = 0.3106(20)$ fm [31], and

$$f(\beta) = (b_0(10/\beta))^{-b_1/(2b_0^2)} \exp(-\beta/(20b_0)), \qquad (3)$$

where $b_0$ and $b_1$ are the universal coefficients of the two-loop beta function.

From $a(\beta)$ we determine, separately for each explored lattice size, $T_c(\mu)/T_c(0) = a(\beta_c(0))/a(\beta_c(\mu))$. Data for
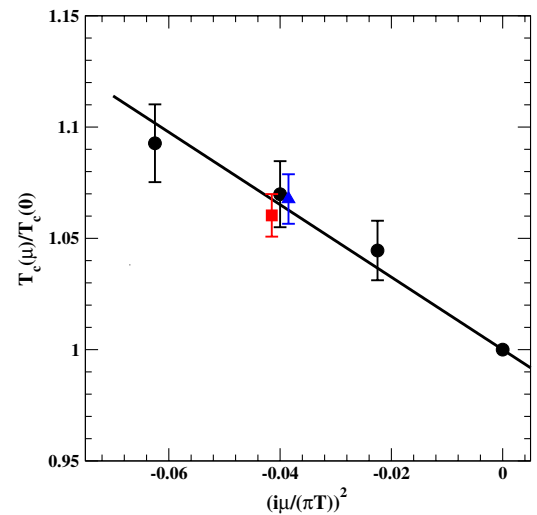


FIG. 2 (color online). $T_c(\mu)/T_c(0)$ versus $((i\mu)/(\pi T))^2$ obtained on a $16^3 \times 6$ lattice (full circles), on a $24^3 \times 6$ lattice (full square), and on a $32^3 \times 8$ lattice (full triangle). For the sake of readability, the abscissae at $((i\mu)/(\pi T))^2 = -0.04$ for $24^3 \times 6$ and $32^3 \times 8$ data have been slightly shifted. The full line is a linear fit to the data on the $16^3 \times 6$ lattice.

$T_c(\mu)/T_c(0)$ versus $\mu/(\pi T)$ are reported in Fig. 2. For the $16^3 \times 6$ lattice, where the determination at three different values of $\mu$ is available, we have tried a linear fit in $\mu^2$:

$$\frac{T_c(\mu)}{T_c(0)} = 1 + R_q \left( \frac{i\mu}{\pi T_c(\mu)} \right)^2, \qquad (4)$$

which works well over the whole explored range ($\chi^2/\text{d.o.f.} = 0.39$) and gives us access to the curvature $R_q$. On the other lattices, assuming that linearity in $\mu^2$ still holds, we can extract $R_q$ from the determination at $\mu/(\pi T) = 0.2i$; we notice that such an assumption, for the given value of $\mu$, is consistent with all previous studies on the systematics of analytic continuation [15–17]. Our results are

$$R_q(16^3 \times 6) = -1.63(22), \qquad \kappa = 0.0183(24),$$
$$R_q(24^3 \times 6) = -1.51(25), \qquad \kappa = 0.0170(28),$$
$$R_q(32^3 \times 8) = -1.70(29), \qquad \kappa = 0.0190(32), \qquad (5)$$

where $\kappa = -R_q/(9\pi^2)$ is the curvature parameter introduced in Eq. (1). The results provide evidence that finite size and finite cutoff systematic effects are within our present statistical uncertainties. We cannot yet try an extrapolation to the continuum limit of our results; however, taking into account the statistical errors and the observed variations of the results with the lattice size and the ultraviolet cutoff, our present estimate for kappa is

$$\kappa = 0.018(4). \qquad (6)$$

## III. CONCLUSIONS AND DISCUSSION

We have presented the first results of our study of QCD with $n_f = 2 + 1$ flavors discretized in the HISQ/tree rooted staggered fermion formulation and in the presence of an imaginary baryon chemical potential, with a physical strange quark mass and a light to strange mass ratio of $m_l/m_s = 1/20$ and $\mu = \mu_l = \mu_s$.

Our main result is an estimate of the curvature of the (pseudo)critical line in the temperature–baryon chemical potential, defined in Eq. (1), which has been obtained by the method of analytic continuation.

It is interesting to compare our estimate with previous lattice results, which have been mostly obtained by the Taylor expansion method, and with the estimates of the freeze-out curve. Such a comparison is performed in Fig. 3. We stress once again that our investigation has been performed with $\mu_l = \mu_s$, as in the numerical setup of Ref. [27], while the other results in Fig. 3 have been obtained for $\mu_s = 0$.

Regarding the freeze-out curve, we report two different estimates. The first is from the analysis of Ref. [2], which is
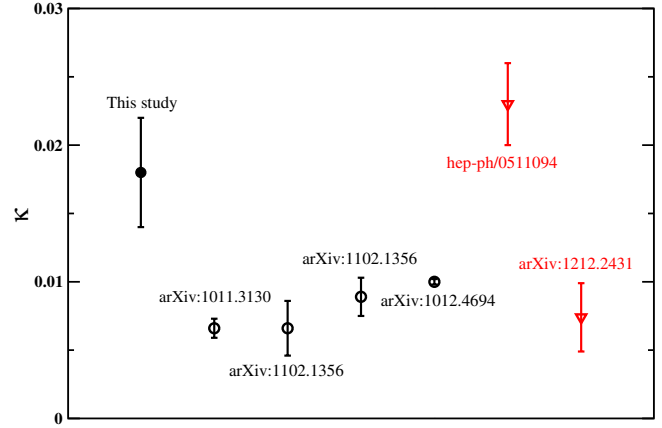


FIG. 3 (color online). Comparison of different determinations of the curvature of the chemical freeze-out curve and of the (pseudo)critical line for QCD with $n_f = 2 + 1$. From left to right: (i) analytic continuation, disconnected chiral susceptibility, this study; (ii) Taylor expansion, chiral susceptibility, Ref. [26]; (iii) Taylor expansion, chiral condensate, Ref. [25]; (iv) Taylor expansion, strange quark number susceptibility, Ref. [25]; (v) analytic continuation, Polyakov loop, Ref. [27]; (vi) freeze-out curvature, standard analysis, Ref. [2]; (vii) freeze-out curvature, revised analysis of Ref. [3].

based on the standard statistical hadronization model; there, the authors parametrize the freeze-out curve as

$$T_c(\mu_B) = a - b\mu_B^2 - c\mu_B^4, \qquad (7)$$

with $a = 0.166(2)$ GeV, $b = 0.139(16)$ GeV$^{-1}$, and $c = 0.053(21)$ GeV$^{-3}$, from which we have derived the $\kappa$ value reported in the figure. The second estimate is based on the estimates for the freeze-out points which are reported in Table I of Ref. [3] and are based on a modified statistical reanalysis of the experimental data which includes the effects of inelastic collisions taking place after freeze-out.

We also report, in Fig. 4, an estimate of the (pseudo) critical line, which is based on our determination of the curvature. Regarding the value of $T_c$ at $\mu_B = 0$, which is affected by larger finite size and finite cutoff effects than $\kappa$, we refer directly to the presently accepted continuum extrapolated value, $T_c \sim 155$ [1,32], and in particular to the one obtained in Ref. [1] with the same action adopted in our study, $T_c(0) = 154(9)$ MeV. From that and from $\kappa = 0.018(4)$ we obtain $b = 0.117(27)$ GeV$^{-1}$ [see Eq. (7)]. Freeze-out determinations from Refs. [2,3] are reported as well.

Our result for the curvature is typically between 2 and 3 standard deviations larger than previous lattice determinations and seems to be in better agreement with the freeze-out curvature based on the standard statistical hadronization model.

Possible reasons for the disagreement with previous lattice determinations can lie in the different methods adopted to avoid the sign problem, in the different lattice
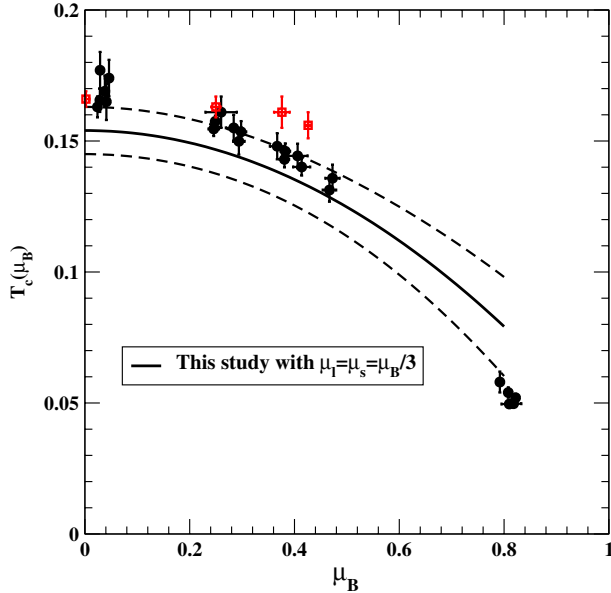
FIG. 4 (color online). $T_c(\mu_B)$ versus $\mu_B$ (units in GeV). Experimental values of $T_c(\mu_B)$ are taken from Fig. 1 of Ref. [2] (circles) and from Table I of Ref. [3] (squares), respectively, for the standard and the modified statistical hadronization model. The solid line is a parametrization corresponding to $T_c(\mu_B) = T_c(0) - b\mu_B^2$, with $T_c(0) = 0.154(9)$ GeV and $b = 0.117(27)$ GeV$^{-1}$. The dashed lines represent the corresponding error band.

imaginary chemical potential with lattice discretizations adopting stout smearing improvement.

Let us conclude by discussing the possible sources of systematic effects in our estimate. One of them is related to the extrapolation from imaginary to real chemical potentials: in the case of the $16^3 \times 6$ lattice, we have performed simulations at different values of imaginary $\mu$, thus verifying that a linear interpolation (in $\mu^2$) of data works well. For the other two lattices, we have instead considered only one value of imaginary $\mu$ ($\mu/(\pi T) = 0.2i$), and the linear behavior has been assumed. Our previous studies based on analytic continuation, however, indicate that the chosen value of $\mu$ should lie well inside the region of linearity. Nevertheless, we plan to perform a more systematic study of this issue. Finally, we have verified that finite size and cutoff effects are under control, within the present statistical accuracy. Still, the extrapolation to the continuum limit, as well as the extension to the physical value of the light to strange mass ratio, $m_l/m_s \sim 1/28$, and the possible effect of varying the strange quark chemical potential deserve further investigations and will be the subject of forthcoming works.

discretizations—as well as in the different observables used to locate the transition point—and in the setup of quark chemical potentials. In this respect, it would be very interesting in the future to redetermine the curvature $\kappa$ using different combinations of methods and lattice discretizations, such as implementing the Taylor expansion method with the HISQ/tree discretization, or the method of

[1] A. Bazavov, T. Bhattacharya, M. Cheng, C. DeTar, H. Ding *et al.*, Phys. Rev. D **85**, 054503 (2012).

[2] J. Cleymans, H. Oeschler, K. Redlich, and S. Wheaton, Phys. Rev. C **73**, 034905 (2006).

[3] F. Becattini, M. Bleicher, T. Kollegger, T. Schuster, J. Steinheimer, and R. Stock, Phys. Rev. Lett. **111**, 082302 (2013).

[4] O. Philipsen, *Proc. Sci.*, LAT2005 (**2006**) 016 [arXiv:hep-lat/0510077]; C. Schmidt, *Proc. Sci.*, LAT2006 (**2006**) 021 [arXiv:hep-lat/0610116]; P. de Forcrand, *Proc. Sci.*, LAT2009 (**2009**) 010 [arXiv:1005.0539]; G. Aarts, *Proc. Sci.*, LATTICE2012 (**2012**) 017 [arXiv:1302.3028].

[5] I. M. Barbour, S. E. Morrison, E. G. Klepfish, J. B. Kogut, and M.-P. Lombardo, Phys. Rev. D **56**, 7063 (1997); Z. Fodor and S. Katz, Phys. Lett. B **534**, 87 (2002).

[6] S. A. Gottlieb, W. Liu, D. Toussaint, R. Renken, and R. Sugar, Phys. Rev. D **38**, 2888 (1988); S. Choe, P. de Forcrand, M. Garcia Perez, S. Hioki, Y. Liu *et al.*, *ibid.* **65**, 054501 (2002); S. Choe *et al.* (QCD-TARO Collaboration), Nucl. Phys. **A698**, 395 (2002); C. Allton, M. Doring, S. Ejiri, S. Hands, O. Kaczmarek, F. Karsch, E. Laermann, and K. Redlich, Phys. Rev. D **71**, 054508 (2005); S. Ejiri, F. Karsch, E. Laermann, and C. Schmidt, *ibid.* **73**, 054506 (2006).

[7] M. G. Alford, A. Kapustin, and F. Wilczek, Phys. Rev. D **59**, 054502 (1999).

[8] A. Hasenfratz and D. Toussaint, Nucl. Phys. **B371**, 539 (1992).

[9] P. de Forcrand and S. Kratochvila, Nucl. Phys. B, Proc. Suppl. **153**, 62 (2006).

[10] G. Bhanot, K. Bitar, and R. Salvador, Phys. Lett. B **188**, 246 (1987); M. Karliner, S. R. Sharpe, and Y. Chang, Nucl. Phys. **B302**, 204 (1988); V. Azcoiti, G. di Carlo, and A. Grillo, Phys. Rev. Lett. **65**, 2239 (1990); J. Ambjorn, K. Anagnostopoulos, J. Nishimura, and J. Verbaarschot, J. High Energy Phys. 10 (2002) 062.

[11] P. de Forcrand and O. Philipsen, Nucl. Phys. **B642**, 290 (2002); Nucl. Phys. **B673**, 170 (2003).

[12] M.-P. Lombardo, Nucl. Phys. B, Proc. Suppl. **83**, 375 (2000); M. D'Elia and M.-P. Lombardo, Phys. Rev. D **67**, 014505 (2003); M. D'Elia and M. P. Lombardo, Phys. Rev. D **70**, 074509 (2004).

[13] V. Azcoiti, G. Di Carlo, A. Galante, and V. Laliena, Nucl. Phys. **B723**, 77 (2005).

[14] P. de Forcrand and O. Philipsen, J. High Energy Phys. 01 (2007) 077; J. High Energy Phys. 11 (2008) 012; P. de Forcrand, S. Kim, and O. Philipsen, Proc. Sci., LAT2007 (**2007**) 178 [arXiv:0711.0262].

[15] P. Cea, L. Cosmai, M. D'Elia, and A. Papa, Phys. Rev. D **81**, 094502 (2010).

[16] P. Cea, L. Cosmai, M. D'Elia, and A. Papa, Proc. Sci., LATTICE2010 (**2010**) 173 [arXiv:1012.4908]; P. Cea, L. Cosmai, M. D'Elia, A. Papa, and F. Sanfilippo, Proc. Sci., LATTICE2012 (**2012**) 067 [arXiv:1210.5896].

[17] P. Cea, L. Cosmai, M. D'Elia, A. Papa, and F. Sanfilippo, Phys. Rev. D **85**, 094512 (2012).

[18] L.-K. Wu, X.-Q. Luo, and H.-S. Chen, Phys. Rev. D **76**, 034505 (2007).

[19] K. Nagata and A. Nakamura, Phys. Rev. D **83**, 114507 (2011).

[20] P. Giudice and A. Papa, Phys. Rev. D **69**, 094509 (2004); Nucl. Phys. B, Proc. Suppl. **140**, 529 (2005).

[21] P. Cea, L. Cosmai, M. D'Elia, and A. Papa, Proc. Sci., LAT2006 (**2006**) 143 [arXiv:hep-lat/0610088]; LAT2007 (**2007**) 214 [arXiv:0710.2068]; LAT2009 (**2009**) 192 [arXiv:1001.4390]; P. CeaL. Cosmai, M. D'Elia, C. Manneschi, and A. Papa, Phys. Rev. D **80**, 034501 (2009); Proc. Sci., LAT2009 (**2009**) 161 [arXiv:1001.4439].

[22] F. Karbstein and M. Thies, Phys. Rev. D **75**, 025003 (2007).

[23] Z. Fodor, Prog. Theor. Exp. Phys. **2012**, 01A108 (2012).

[24] Y. Aoki, S. Borsanyi, S. Durr, Z. Fodor, S. Katz, and K. K. Szabo, Nucl. Phys. **A830**, 805c(2009).

[25] G. Endrodi, Z. Fodor, S. Katz, and K. Szabo, J. High Energy Phys. 04 (2011) 001.

[26] O. Kaczmarek, F. Karsch, E. Laermann, C. Miao, S. Mukherjee, P. Petreczky, C. Schmidt, W. Soeldner, and W. Unger, Phys. Rev. D **83**, 014504 (2011).

[27] R. Falcone, E. Laermann, and M. P. Lombardo, Proc. Sci., LATTICE2010 (**2010**) 183 [arXiv:1012.4694].

[28] E. Follana, Q. Mason, C. Davies, K. Hornbostel, G. Lepage, J. Shigemitsu, H. Trottier, and K. Wong (HPQCD Collaboration, UKQCD Collaboration), Phys. Rev. D **75**, 054502 (2007).

[29] A. Bazavov et al. (MILC Collaboration), Phys. Rev. D **82**, 074501 (2010).

[30] http://www.physics.utah.edu/~detar/milc/.

[31] A. Bazavov et al. (MILC Collaboration), Proc. Sci, LATTICE2010 (**2010**) 074 [arXiv:1012.0868].

[32] Y. Aoki, Z. Fodor, S. Katz, and K. Szabo, Phys. Lett. B **643**, 46 (2006); Y. Aoki, S. Borsanyi, S. Durr, Z. Fodor, S. D. Katz, S. Krieg, and K. Szabo, J. High Energy Phys. 06 (2009) 088; S. Borsanyi, Z. Fodor, C. Hoelbling, S. D. Katz, S. Krieg, C. Ratti, and K. K. Szabó (Wuppertal-Budapest Collaboration), J. High Energy Phys. 09 (2010) 073.